A LIGHT-WEIGHT INFLATABLE HYPERSONIC DRAG DEVICE FOR PLANETARY ENTRY

Angus D. McRonald,*
Jet Propulsion Laboratory
California Institute of Technology

ABSTRACT

The author has analyzed the use of a light-weight inflatable hypersonic drag device, called a ballute, (balloon + parachute) for flight in planetary atmospheres, for entry, aerocapture, and aerobraking. Studies to date include missions to Mars, Venus, Earth, Saturn, Titan, Neptune and Pluto. Data on a Pluto lander and a Mars orbiter will be presented to illustrate the concept. The main advantage of using a ballute is that aero deceleration and heating in atmospheric entry occurs at much smaller atmospheric density with a ballute than without it. For example, if a ballute has a diameter 10 times as large as the spacecraft, for unchanged total mass, entry speed and entry angle, the atmospheric density at peak convective heating is reduced by a factor of 100, reducing the peak heating by a factor of 10 for the spacecraft, and a factor of about 30 for the ballute. Consequently the entry payload (lander, orbiter, etc.) is subject to much less heating, requires a much reduced thermal protection system (possibly only an MLI blanket), and the spacecraft design is therefore relatively unchanged from its vacuum counterpart. The heat flux on the ballute is small enough to be radiated at temperatures below 800 K or so. Also, the heating may be reduced further because the ballute enters at a more shallow angle, even allowing for the increased delivery angle error. Added advantages are a smaller mass ratio of entry system to total entry mass, and freedom from the low-density and transonic instability problems that conventional rigid entry bodies suffer, since the vehicle attitude is determined by the ballute, usually released at continuum conditions (hypersonic for an orbiter, and subsonic for a lander). Also, for a lander the range from entry to touchdown is less, offering a smaller footprint. The ballute derives an entry corridor for aerocapture by entering on a path that would lead to landing, and releasing the ballute adaptively, responding to measured deceleration, at a speed computed to achieve the desired orbiter exit conditions. For a lander an accurate landing point could be achieved by providing the lander with a small gliding capacity, using the large potential energy available from being subsonic at high altitude. Alternatively the ballute can be retained to act as a parachute or soft-landing device, or to float the payload as a buoyant aerobot. As expected, the ballute has smaller size for relatively small entry speeds, such as for Mars, or for the extensive atmosphere of a low-gravity planet such as Pluto. The author will discuss presently available ballute materials and a development program of aerodynamic tests and materials that would

* A. D. McRonald is a Member of the Technical Staff at the Jet Propulsion Laboratory of the California Institute of Technology. His opinions are his own. This work was performed at the Jet Propulsion Laboratory and was funded by NASA. The paper was presented at the Association Aeronautique et Astrounatique de France Conference at Arcachon, France on March 16-18, 1999. Email: angus@bruno.jpl.nasa.gov

be required for ballutes to achieve their full potential.

INTRODUCTION

A hypersonic drag device was first studied in the late sixties by the Goodyear Company in Ref. 1, and at Langley RC by NASA in Ref. 2, one objective being to assist the Viking landers decelerate during Mars entry. For the Viking task wind tunnel tests were performed on two shapes, for which stability was a prime consideration. The drag device, called a ballute, was to be inflated at modest hypersonic speed some time after peak heating and deceleration. The ballutes were heavy and were inflated at relatively low speed and high pressure.

A ballute inflated prior to entry was first studied in Ref. 3, which proposed to use a ballute to decelerate during entry into Venus. One heavy ballute, weighing several hundred kilograms, was inflated prior to entry, released after deceleration, and replaced by another ballute used as an aerobot or buoyant platform. The authors of Ref. 3 evaluated the convective heating rate and its time integral, and computed how much material was ablated from the entry ballute. They also compared several candidate materials for the entry ballute. In recent years many materials have become commercially available in very thin sheets, and some will take relatively high temperatures, such as Kapton, up to 500 C, and PBO (Polyboxoxazole, a liquid crystal polymer), up to 600 C.

PRESENT STUDIES

The author made a first study of a ballute for direct entry of a Neptune orbiter in 1994, as an alternative to use of a conventional lifting vehicle. Trajectories were computed for various entry angles and ballute sizes. It became apparent that an entry corridor for aerocapture could be created by releasing the ballute when sufficient delta-V had been reached during an atmospheric pass. After release the orbiter would fly on to exit the atmosphere with relatively little further delta-V. One can see that in a convective heating situation the heating rate decreases greatly when a ballute is used. For example, if the ballute diameter is ten times that of the orbiter, the density at which peak deceleration or peak heating is reached is reduced by a factor of 100, so that the convective heating rate to both the orbiter and the ballute is thereby reduced by a factor of 10. For the ballute an additional reduction of square root of 10, about 3.1 comes from the large size, and a further reduction is probable for both orbiter and ballute, due to the entry angle being reduced, and the altitude being much greater, likely to be in a region where the scale height is greater. One can note also that even for radiative heating there is a reduction relative to the orbiter aerocapturing in a lifting body, since the above reduction of 100 in density when a ballute is used reduces the radiative heating more than the large ballute size increases it. The reduction in heating applies equally to the case of entry, and here the ballute decelerates the lander at much higher altitude than the conventional rigid body entry vehicle. Thereafter the ballute may be released to achieve a rapid descent, or may be retained to achieve a soft landing, or, if the ballute is filled with He, can become a buoyant vehicle prior to landing. Since

1994 studies have been made of ballutes for aerocapture and entry into the planets Mars, Venus, Earth, Saturn and Pluto and the moon Titan. Details of a Mars orbiter and a Pluto lander will be presented to illustrate the process.

The deceleration assumes constant hypersonic C_d for the initial entry with the ballute attached, and then for the orbiter flight after ballute release. The basic deceleration equation is:

$$\frac{dV}{dt} = 0.5 V_a^2 / \left(m / C_d A \right) \qquad (1)$$

where V_a is the velocity, T is time, C_d is the constant drag coefficient, A is the cross section area, $p/4 * D^2$, D is the diameter and m is the mass. The equation applies to both ballute + orbiter and to orbiter alone, with the appropriate values of m, C_d, D and A.

BALLUTE SHAPE

The first shape considered was a sphere, for which the flow features are relatively simple and understood. The sphere may be inflated out of an orbiter, as shown in Fig. 1,a, which has the advantage that the heating on the orbiter is the same as the ballute, but has inconvenience in the vehicle layout and in ballute release. A sphere let out astern on a tether, as in Fig. 1(b) is more convenient, having little impact on orbiter design, and making ballute release easy. The leading face and the corners of the orbiter require thermal protection with MLI (multi-layer insulation) of some nature. The ballutes shown in Fig. 1 show a net enclosing them, to take the substantial aerodynamic drag force. A more efficient shape in terms of drag per unit mass is shown in Fig, 1(c) somewhat like a fat lens. The drag coefficient, C_d is about 2, compared with 0.9 for a sphere, and the ballute material mass is about one half, so that a lens-shape ballute for a given task will be about one half the diameter of a spherical ballute. A further reduction of ballute mass could be achieved by replacing the lens shape by a disk, i.e., only one layer of material. Both the lens shape and the disk require some help in deployment, possibly using inflatable tubing stretching from the orbiter as shown, and including a circumferential ring. Although the lens and the disk hold out the prospect of lower mass and higher C_d, they have some more complex configurations to be analyzed. Also, the total mass of the ballute is made up of a net enclosing the ballute, to take the substantial aerodynamic drag force, the fabric of the ballute, and gas to inflate the volume of the sphere and the lens, and also the tubing. These vary differently with radius R: the net as R, the fabric as R squared, and the inflation gas as R cubed, so that the variation of total mass is a mix that depends on size. For a very large entry mass the ballute radius R would become large enough for the R cubed term to become significant or dominant. For smaller ballutes the fabric term varying as R squared is usually the main mass.

MARS ORBITER TRAJECTORIES

For the atmospheric pass for direct entry of a micro-mission Mars orbiter, with entry mass about 100 kg, the basic approach was to evaluate a number of entry

trajectories for different constant values of ballistic coefficient, $B = m/C_dA$, where m is the entry mass, C_d is the hypersonic drag coefficient (0.9 for a sphere) and A is the frontal area. Trajectories were run for 7 values of B, = 5, 2.5, 1.0, 0.5, 0.25 and 0.1 kg/m^2, and the delta-V loss for a complete pass (no ballute release) is shown in Fig. 2 as a function of the entry angle, gamma. The entry speed was 5.5 km/s at altitude 125 km, and the COSPAR nominal atmosphere model was used. Aerocapture into an elliptic orbit required a delta-V of between about 500 and 2000 m/s, shown by the horizontal lines in Fig. 2. If the delta-V loss is less than about 500 m/s the vehicle will exit in a hyperbolic trajectory. If the delta-V loss is more than about 2000 m/s the vehicle will enter, or possibly skip out but re-enter. The mission designer usually seeks a fairly close circular orbit, so that the target delta-V is probably a little below 2000 m/s. The amount by which the target delta-V differs from 2000 m/s will depend on the errors expected in entry angle and the extent to which the atmospheric density departs from the model used., and the ability of the ballute release system to predict the delta-V at exit. A burn at the first apoapsis is necessary to lift the periapse out of the atmosphere. Because of delivery error, computed to be about 0.25 deg at the 2 sigma level, and possible variation in the atmosphere, one needs an entry corridor of about 0.6 deg from one side to the other to accomplish aerocapture with certainty. Figure 2 shows the delta-V for a complete atmospheric pass of the ballute, whereas in actuality it is released when onboard deceleration readings indicate that a chosen delta-V will be achieved by the orbiter at exit.

This concept is shown in more detail in Fig. 3, which shows the speed V as a function of entry angle, gamma, for five of the vehicle sizes. The group of curves marked (l) and (2) near the top of Fig. 3 show the velocity V at maximum deceleration, g_{max}, and the value of V at minimum altitude, respectively. The vehicle number is marked on the trajectories. The remaining groups of curves, marked (3), (4) and (5) all refer to exit values of V respectively for the cases: (3) for ballute release at V = 4100 m/s in the pass, as determined by the measured time-integrated deceleration; (4) for ballute release at V = 3700 m/s, and (5) for no ballute release. For (3) and (4) the slope of the V at exit with entry angle is much less steep than when the ballute is retained; the $B = m/|C_dA$ of the orbiter after ballute release was assumed to be 30 kg/m^2; this value is probably about half the value for the orbiter alone, and it has been assumed here that the orbiter will have some part of the ballute deliberately retained to give it a stable attitude in the remainder of the atmospheric pass, or has a skirt of some kind for the same purpose. One can see that an entry angle corridor width of 0.6 deg or more, as mentioned above, is achieved for vehicles number 3, 4 and 5, releasing the ballute at 4100 m/s. One wishes a small slope of the V exit value with angle gamma, so that a high B of the orbiter is desirable. In fact, an accurate ballute exit V is achieved by two steps: (1) measure the actual delta-V loss as a function of time, and (2) estimate the post-release orbiter delta-V loss on the basis of the onboard determination of the apparent nominal gamma, and release at the adaptive

delta-V loss designed to achieve accurate exit conditions.

The peak g-load for the ballutes is shown versus entry angle in Fig.4, and Fig. 5 shows the peak stagnation pressure and the peak reference convective heating rate, $qref_{max}$, versus entry angle.

The reference heating parameter qref assumed in these calculations is the convective heating rate to the stagnation point of a sphere of radius 0.43 m. The equations for the peak pressure and peak reference heating for the ballute are of the form:

$$pressure \qquad p = \rho V^2 \tag{2}$$

$$convectiveheatingrate \; q_{ref} = const.\rho^{1/2} V^3 \tag{3}$$

where rho is the atmospheric density.. The Knudsen number Kn of the flow was evaluated. At peak deceleration Kn is about 0.01 for the ballute and about 0.1 for the orbiter, so that the orbiter is in transitional flow and the ballute is in low Reynolds number continuum flow. The tube and tether are probably in free-molecular flow. The peak ballute temperature is evaluated from a balance of radiation from the ballute stagnation point, both outwards and inwards, and the incident convective heating rate.

Temperature T: (4)

$$T^4 = \frac{1}{2(5.67)\varepsilon}\left(\frac{0.43}{R}\right)^{1/2} \frac{q_{ref}}{5.67} * 1000.$$

where ε is the emissivity.

BALLUTE SIZE, MASS

To determine the ballute size corresponding to a value of $B = m/C_dA$, we assume a mass m of 100 kg, and taking the hypersonic C_d for a sphere as 0.9, we can find the values of radius R for the seven sizes studied. From R we can compute the actual $qref_{max}$, and hence the maximum temperature, assuming the ballute material to radiate on both sides with an assumed emissivity, reaching equilibrium almost instantly with the external convective stagnation point heating. Two materials were studied: Kapton, assumed to have an emissivity of 0.5 and a mass/area of 10 gm/m^2, equivalent to a thickness of 7 micron, and PBO, assumed to have an emissivity of 0.7, and a mass/area of 20 gm/m^2, equivalent to about 14 micron thickness. The data are from Ref. 4. The ballute was presumed to be pressurized to 50 N/m^2, the maximum external stagnation pressure, and to have a net made of PBO, for which a tensile strength of 56 kgf/mm^2 was assumed—the value at room temperature. The maximum total force to be taken by the net was the entry mass (more exactly the orbiter mass, almost the same) times the maximum g-load. With these assumptions one can compute the masses of the ballute, the net, the He gas, the gas bottle, assumed to be the same mass as the He, and the maximum temperature of the stagnation point of the ballute. These steps were performed for the 7 ballutes with assumed entry mass of 100, 400 and 1600 kg. The maximum temperatures, T_{max}, are shown for the 7 trajectories in Fig. 6, and Fig. 7 shows the mass fraction versus radius for the ballutes with entry mass 100, 400 and 1600 kg.

The dashed lines connect points of T_{max} = 200, 300, 400, 500 and 600 C. These mass values have no margin and do not include several ballute related masses, e.g., a container for the ballute and a release device, as well as a design margin, so that real project masses would be considerably higher. One can see that a 100 kg orbiter with 10 gm/m^2 Kapton sphere would have a radius of about 6 m. at about a peak temperature of 450 C.

PLUTO LANDER

The same ballute concept has been applied to a Pluto lander, as illustrated in Fig. 8, which shows entry trajectories at Pluto for a ballute with B = m/C_dA of 0.05 kg/m^2, and an entry speed of 15 km/s. The atmosphere model was constructed by Russian engineers working with the Pluto Express group at JPL, for the year 2013, based on star occultation measurements by MIT scientists in 1988, and having a surface pressure of 3 microbars. Because of the low gravity the atmosphere extends out to 700 km, the chosen entry point, and the entry angles are in the range 48 to 56 deg. With this value of B one can find a trajectory which decelerates to about 100 m/s at surface impact, i.e., in the range of penetrator impact speeds.

Figures 9, 10, and 11 show, respectively the peak g-load, the peak stagnation point pressure, and the peak reference convective heating rate versus entry angle in the range 44 to 58 deg, at altitude 700 km. It can be seen that, although the maximum pressure for Pluto entry is not much more than for the Mars orbiter, the g-loads are much larger, about 20, than for the Mars orbiter (about 3), because the ballute is larger. Consequently, the net will become a greater mass fraction for Pluto.

Figure 12 shows the temperature versus time from entry for three values of B = m/C_dA at entry angle 52 deg., for an entry mass m = 60 kg. For a given entry mass, one can see that the peak temperature decreases for a larger ballute, but then the mass of the ballute system increases, and may consume all the assumed entry mass. The mass fraction was computed for a range of entry angles 48 to 58 deg, two entry masses, 30 and 60 kg, and for two shapes: a sphere at 10 gm/m^2, and a blunt lens shape at 20 gm/m^2 (PBO) and 10 gm/m^2 (Kapton). The results are shown in Fig. 13. One can see that ballutes with B = 0.1 and 0.05 kg/m^2 are feasible with a payload fraction over 50%. A 30 kg ballute with B = 0.1 kg/m^2 and a blunt lens shape has a radius of 6.9 m. A disk shape would give about the same performance with a radius of about 4.9 m.

CAVEATS

The forces and temperatures predicted for these ballutes are theoretical, and require flight validation. There may be flow instabilities, leading to rapid motions harmful to the ballute materials. The flow regime, Knudsen numbers about 0.01 on the ballute, about 0.1 on the orbiter, make it uncertain to what extent the orbiter wake closes before reaching the ballute. Suggested tests that could cast light on the behavior of the system in flight include ground tests with the same drag force to model shape changes, sounding rocket flights to achieve supersonic conditions,

deployment and entry tests from an Ariane piggyback opportunity, and deployment and entry tests out of the STS. Video camera, accelerometers, pyrometers, color change paints, and film temperature gauges are appropriate instrumentation, and also ground tracking.

CONCLUSIONS

Entry ballutes have been studied for a Mars orbiter and for a Pluto lander, and the conclusions are that the concept offers advantages in mass fraction and flexibility of mission design over conventional entry vehicles and lifting vehicles for aerocapture. The studies indicate, for example, that one can design a spherical ballute of radius about 6 m for a 100 kg Mars orbiter, and a blunt lens shape of ballute for a Pluto lander of radius about 6 m, for an entry mass of 30 kg, with about 50% payload. If the concepts described here prove to be feasible in practical flight it would become easier to design and implement atmospheric flights such as aerocapture and entry.

REFERENCES

1. I. M. Jahemenko, "Ballute Characteristics in the 0.1 to 10 Mach Number Speed Range," J. Spacecraft, Vol. 4, No. 8, 1058-63, August, 1967.
2. L. D. Guy, "Structural and Decelerator Design Options for Mars Entry," J. Spacecraft, Vol. 6, No. 1, 44-49, January 1969.
3. H. Akiba et al., "Feasibility Study of Buoyant Venus Station Placed by Inflated Balloon Entry," Paper at the 27th Int. Conf. Astronomy, Anaheim, Calif., Oct., 1976.
4. A. Yavrouian et al., "High Temperature Materials for Venus Balloon Envelopes," AIAA Paper, 1995.

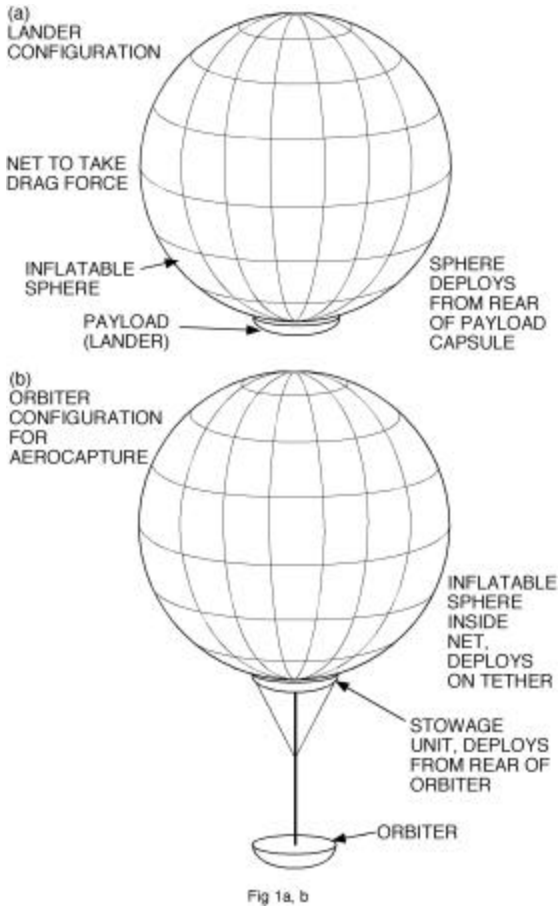

Figure 1: Ballute Shapes: (a) sphere: lander configuration; (b) sphere: orbiter configuration

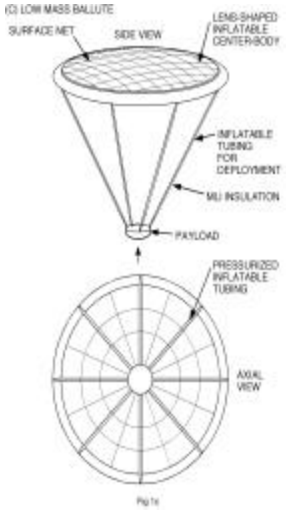

Figure 1: (c) lens shape, for reduced mass and size.

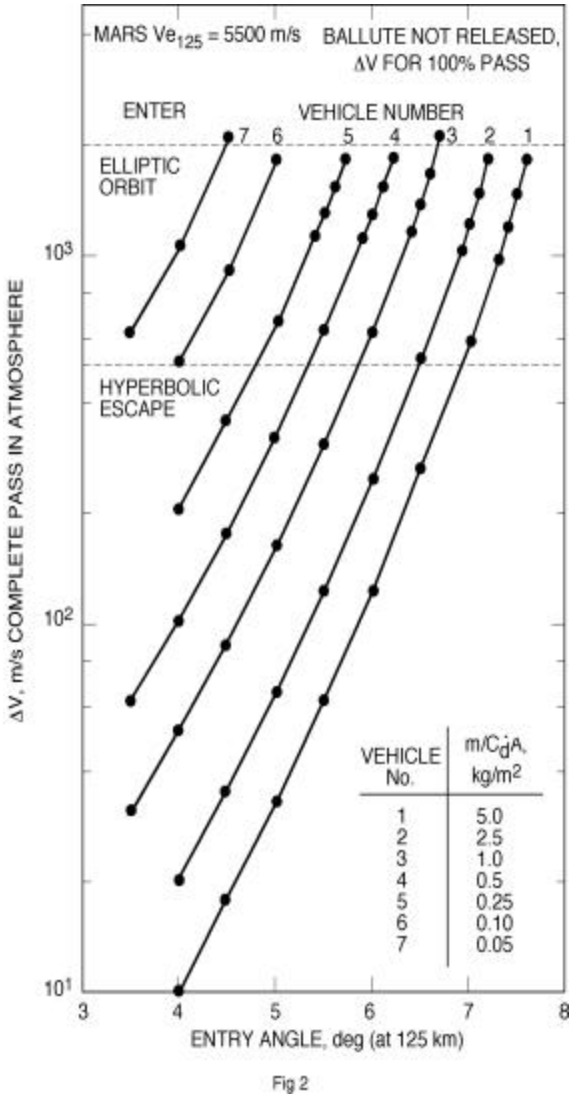

Figure 2. Delta-V loss for 7 ballute sizes versus entry angle.

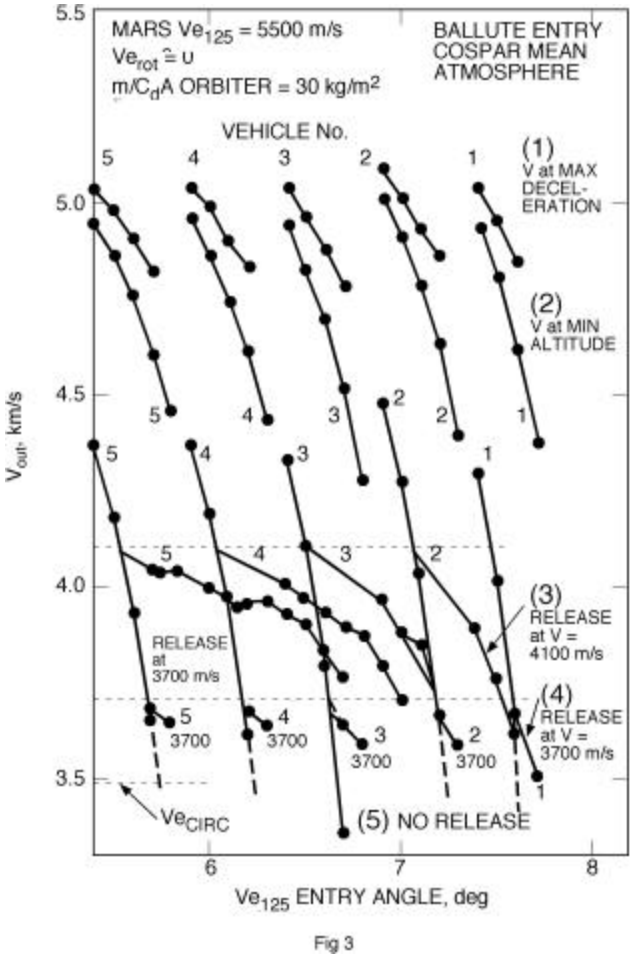

Figure 3. Velocity V versus entry angle for 5 of the ballute sizes: (1) circled shows velocity V at maximum deceleration; (2) shows V at minimum altitude; (3) and (4) show exit V for ballute release at 4100 m/s and 3700 m/s, respectively; (5) shows exit V when ballute is not released.

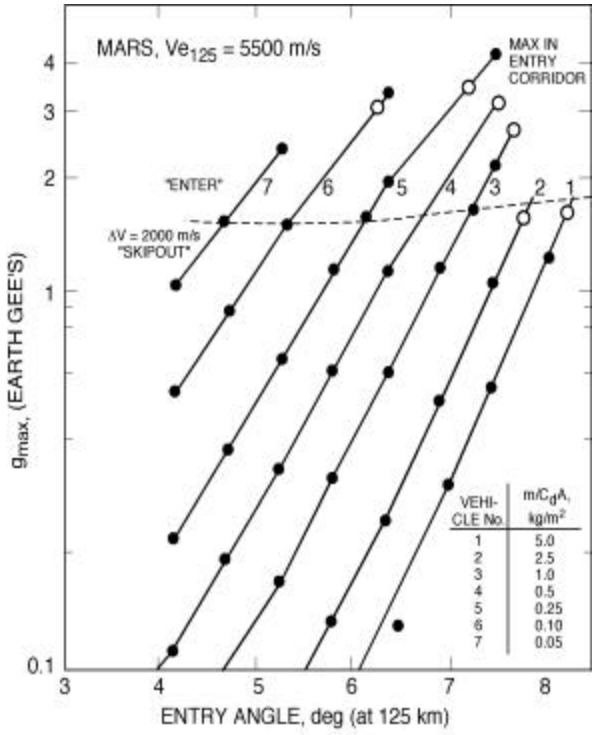

Figure 4. Peak g-load versus entry angle for the 7 ballutes.

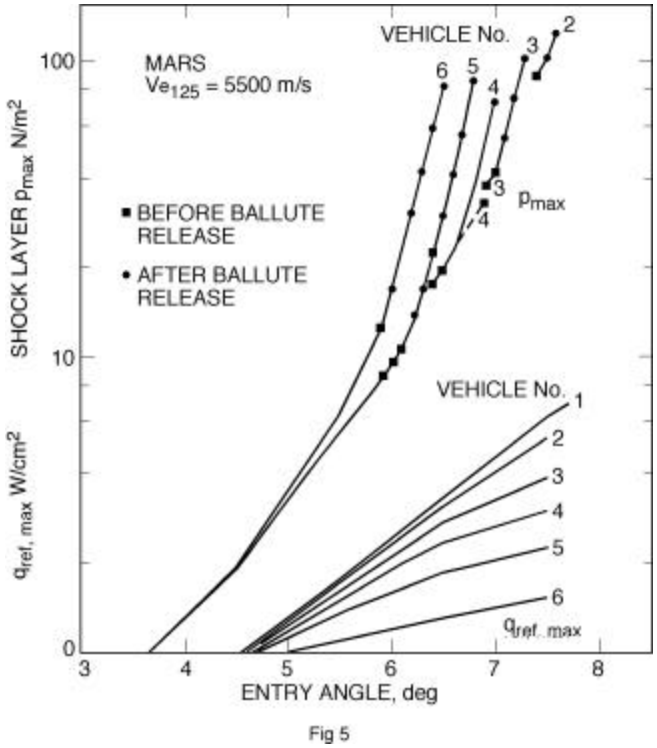

Figure 5. Peak stagnation pressure and peak reference convective heating rate for the ballutes versus entry angle.

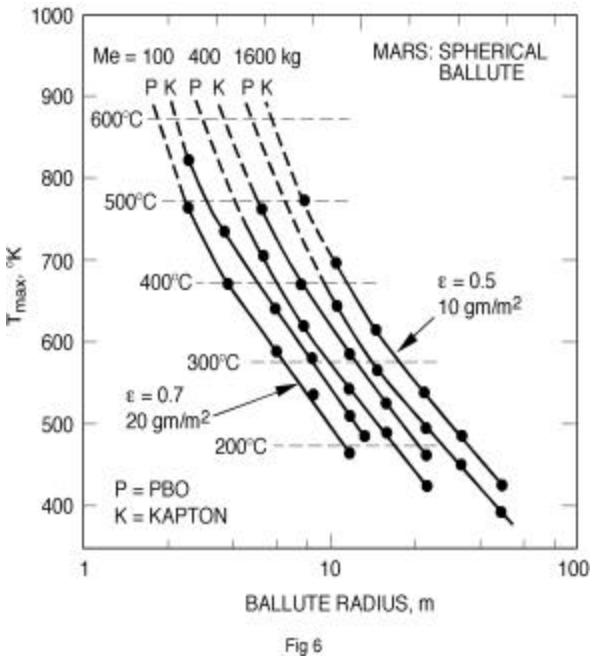

Figure 6. Peak temperature for the ballutes versus ballute radius, for PBO and Kapton, for entry mass values of 100, 400 and 1600 kg.

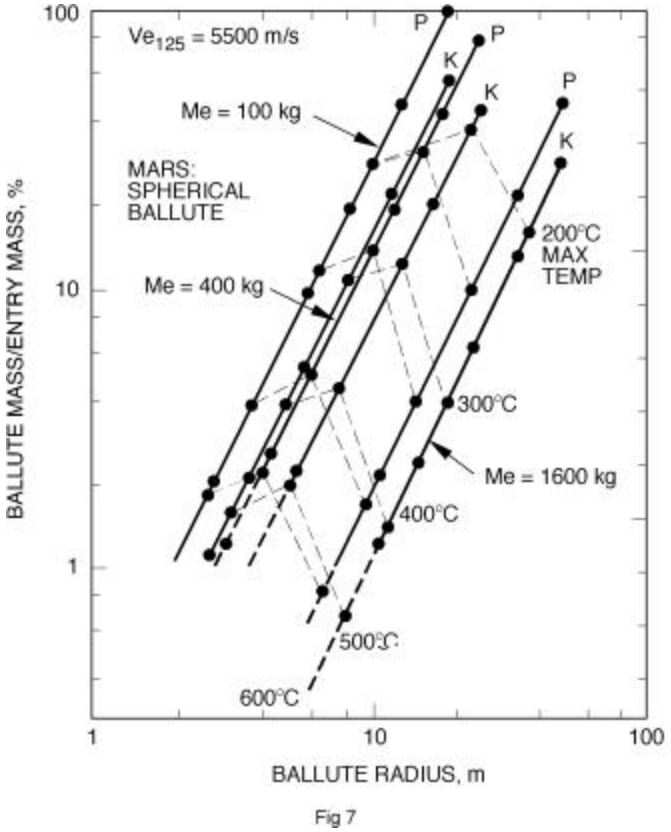

Figure 7. Mass fraction of the ballute system (net, ballute, gas, bottle) versus ballute radius, for PBO and Kapton, for entry mass 100, 400 and 1600 kg.

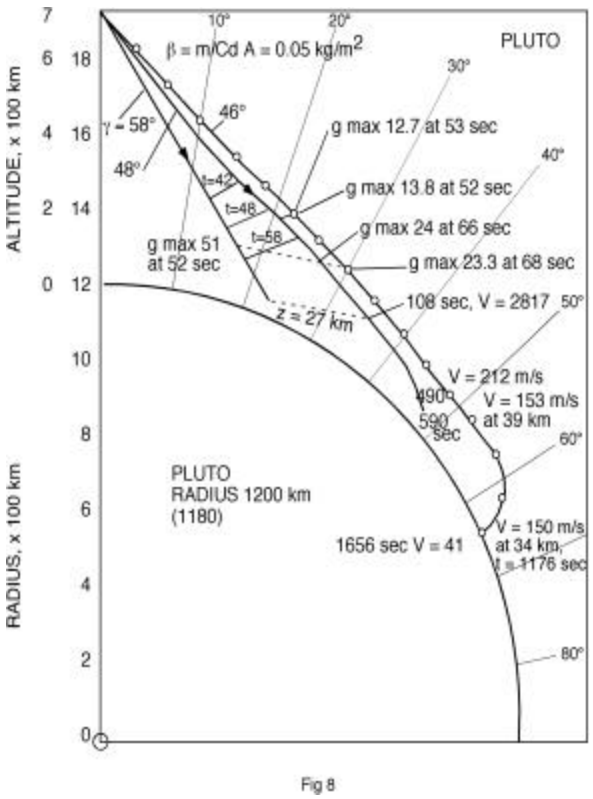

Fig 8

Figure 8. Entry trajectories at Pluto for entry angles 46, 48 and 56 deg, at entry speed 15 km/s, and B = m/C_dA = 0.05 kg/m^2.

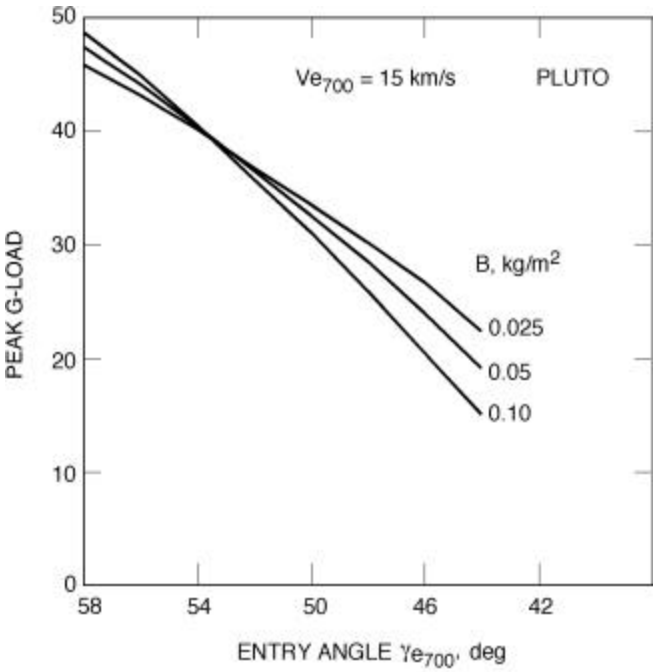

Fig 9

Figure 9. Peak g-load for Pluto entry versus entry angle, for ballutes with m/C_dA = 0.025, 0.05 and 0.10 kg/m^2.

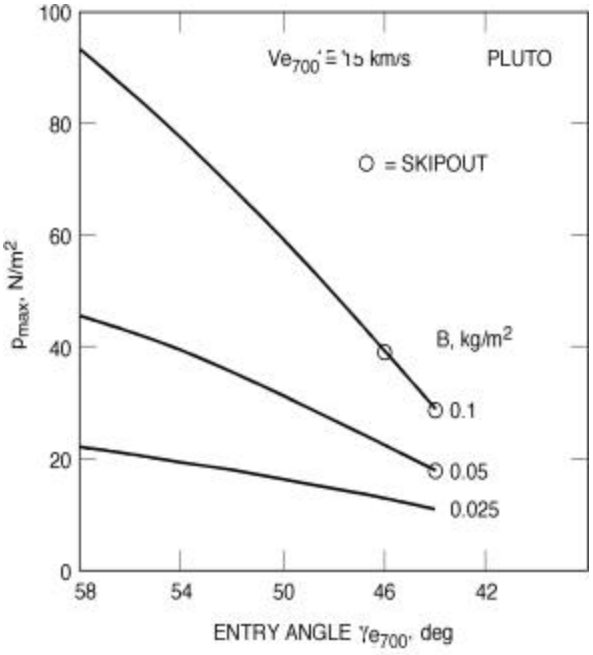

Figure 10. Peak stagnation point pressure for Pluto entry versus entry angle, for ballutes with m/C_dA = 0.025, 0.05, and 0.1 kg/m^2.

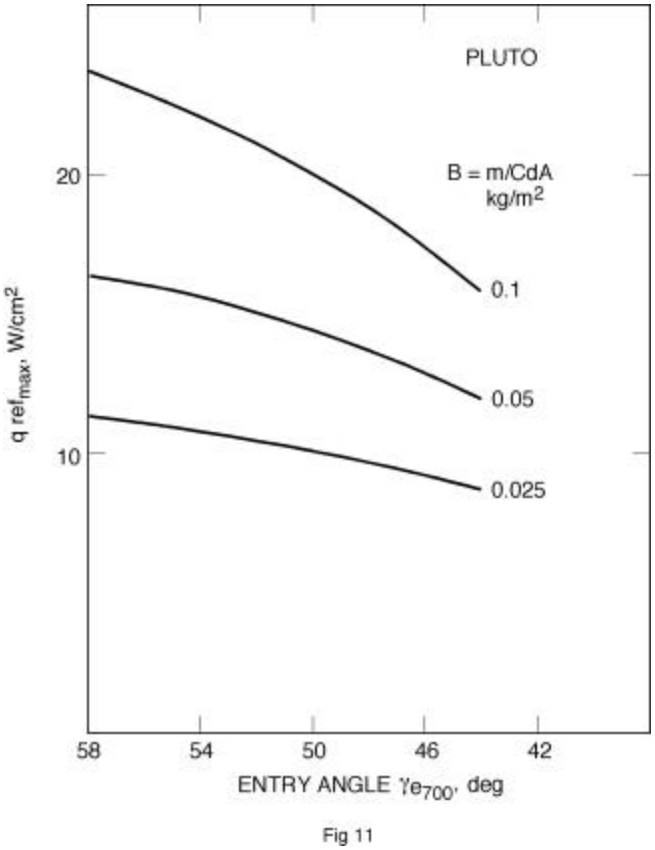

Figure 11. Peak reference stagnation point heating rate, $qref_{max}$ versus entry angle, for ballutes with m/C_dA = 0.025, 0.05 and 0.10 kg/m^2.

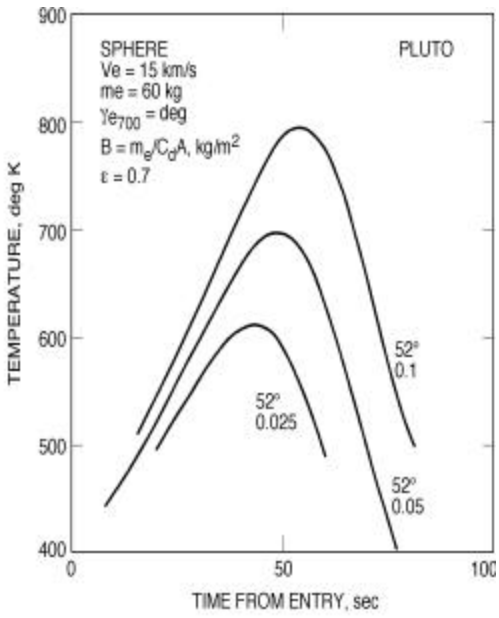

Fig 12

Figure 12. Temperature versus time from entry for entry angle 52 deg, entry mass 60 kg and m/C_dA = 0.025, 0.05 and 0.10 kg/m^2.

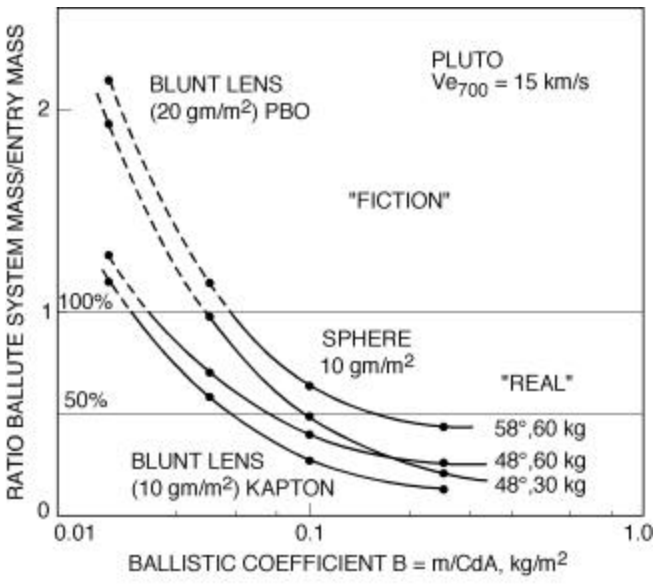

Fig 13

Fig. 13. Mass fraction: ratio of ballute system mass to entry mass, for entry mass 60 and 30 kg, Kapton sphere, and Kapton and PBO lens shape.